PHYSICAL REVIEW B VOLUME 26, NUMBER 12 15 DECEMBER 1982

Electronic structure of $NiSi_2$

Yu-Jeng Chang and J. L. Erskine
Department of Physics, The University of Texas at Austin, Austin, Texas 78712
(Received 7 April 1982)

Structural and electronic properties of epitaxial $NiSi_2$ crystals are investigated with the use of low-energy-electron diffraction, Auger spectroscopy, and photoemission. Normal emission spectra from (111) and (100) $NiSi_2$ surfaces yield band dispersions and critical-point energies along Γ-L and Γ-X directions of the bulk Brillouin zone which support the results of recent self-consistent band calculations. No evidence of surface reconstruction is observed on (111) or (100) $NiSi_2$ crystal faces; however, high-temperature annealing does promote silicon-atom segregation at the surface.

Widespread application of silicide interfaces in semiconductor devices has stimulated recent work on the basic physical properties of metal semiconductor compounds. Nickel silicides are particularly interesting because of certain metallurgical properties: Several stable stoichiometric nickel silicon compounds form,[1] thus permitting studies in which the alloy composition is a variable parameter. Planar nickel silicides exhibit selective growth[2] and, in addition, the silicon-rich silicide phase $NiSi_2$ forms an extremely abrupt interface[3] when produced by reacting a nickel film with a Si(100) surface. This epitaxial structure offers attractive prospects of conducting detailed investigations of interfaces using electron spectroscopy. Additional motivation for studying nickel silicides has recently been furnished by self-consistent calculations[4,5] of their electronic structure which provide a detailed framework for analyzing experimental results. In this paper we report low-energy-electron diffraction (LEED), Auger and photoemission studies of the structure and electronic properties of $NiSi_2$. Our results support conclusions of recent theoretical work and yield critical-point binding energies for several bands along Γ-L and Γ-X directions of the bulk Brillouin zone.

Rutherford backscattering and channeling studies[3] have shown that $NiSi_2$ films with excellent epitaxial structure can be grown on Si surfaces. Oriented crystalline formation is aided by a nearly perfect match of the $NiSi_2$ bulk lattice parameter to the Si lattice parameter. Reflection electron diffraction studies[6] have shown that the $NiSi_2$ epitaxial layer orientation is the same as the substrate, and our x-ray Laue and LEED studies of epitaxial silicides formed on Si(100) and (111) also support these results.

Our $NiSi_2$ samples were prepared by vacuum evaporating Ni films ($\lesssim 1000$ Å thick as determined by a calibrated quartz microbalance) on lightly doped p-type silicon crystals furnished by Monsanto. Prior to film deposition, the Si(111) and (100) surfaces were cleaned by cycles of argon ion sputtering (500 eV, 10 μA/cm^2) and annealing at 800 °C. This cleaning procedure produced sharp (7×7) LEED patterns for Si(111) surfaces, sharp (2×1) LEED patterns for Si(100) surfaces, and the expected surface states[7] which were observed using angle-resolved ultraviolet photoemission spectroscopy (ARUPS). After *in situ* film deposition and annealing at 800 °C for 30 min, sharp (1×1) LEED patterns were observed for both (111) and (100) crystal faces, and Auger spectroscopy revealed only Si and Ni lines indicating the formation of ordered silicide compounds with no surface reconstruction. Annealing the films at 800 °C insures the Si-rich compound $NiSi_2$ is formed.[2]

The primary objective of the work reported here was to study the bulk electronic properties of $NiSi_2$. Previous studies of thin-film silicides have shown that annealing processes required to form silicide compounds on silicon surfaces can also produce significant segregation at the silicide phase surface.[8] Surface segregation and related effects are particularly likely to be important for the $NiSi_2$ phase because relatively high temperatures (800 °C) are required to produce this stoichiometry. In order to determine the extent that surface segregation, island formation, and related phenomena affected our results, Auger spectroscopy, work function measurements, and LEED were used to investigate the effects of annealing and argon ion sputtering on our ARUPS data.

We found that prolonged high-temperature annealing (850 °C) of either (111) or (100) silicide surfaces decreased the Ni (848 eV) to Si (91 eV) peak-to-peak ratio in Auger spectra. The work function also decreased slightly from values we judged as representing virgin $NiSi_2$ surfaces. These work function values are $NiSi_2(100)$, $\phi = 5.03 \pm 0.05$ eV and $NiSi_2(111)$, $\phi = 5.05 \pm 0.05$ eV.[9] Typical annealing-induced changes were $\Delta\phi \sim 0.2$ eV. The change in Auger peak ratio is consistent with the conclusion that silicon segregates at the surface. This segregation did produce minor changes in our ARUPS spectra. The primary effect was a slight decrease in d-state emis-

sion features. These effects can be practically eliminated by a few minutes of sputtering (500 eV, 10 $\mu A/cm^2$) followed by brief annealing to 500 °C.

Angle-resolved photoelectron energy distribution curves were obtained using a spectrometer which has been described previously.[10] Base pressures were maintained in the 10^{-11}-Torr range, and pressures during evaporation and during resonance lamp operation were typically in the 10^{-10}-Torr range. All measurements were made with the sample at room temperature and with an analyzer angular resolution $\Delta\Omega = 4°$. Electron spectrometer resolution ΔE_s for the four lower photon energies, $\hbar\omega \leq 26.85$ eV, was maintained at $\Delta E_s \approx 100$ meV; for $\hbar\omega \geq 40.82$ eV, $\Delta E_s \approx 200$ meV.

Figure 1 displays normal emission energy distribution curves (EDC's) for $NiSi_2(111)$. Peaks and other features are identified by letters and the corresponding binding energies measured from the Fermi level E_F are tabulated. Resonance line energies (shown to the right of each EDC) were used to determine the Fermi energy for each curve in relation to the Fermi energy of the 21.22-eV spectra. Figure 2 displays corresponding normal emission EDC's for

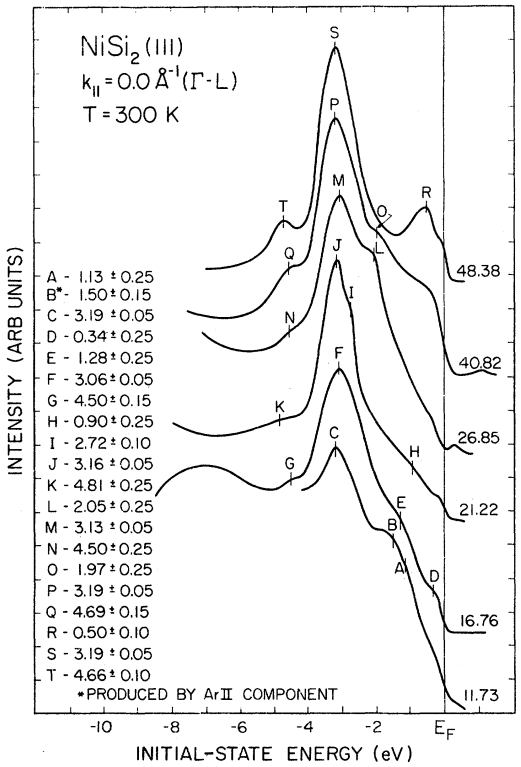

FIG. 1. Angle-resolved photoelectron energy distribution curves for $NiSi_2(111)$. Data were taken in normal emission geometry with $\Delta\Omega = 4°$. Energy resolution: $\hbar\omega = 43.88$ and 40.82 eV, $\Delta E_S \approx 200$ meV; other $\hbar\omega$, $\Delta E_s \approx 100$ meV. (Refer to Ref. 16 and text for a discussion of the origin of peak *B*.)

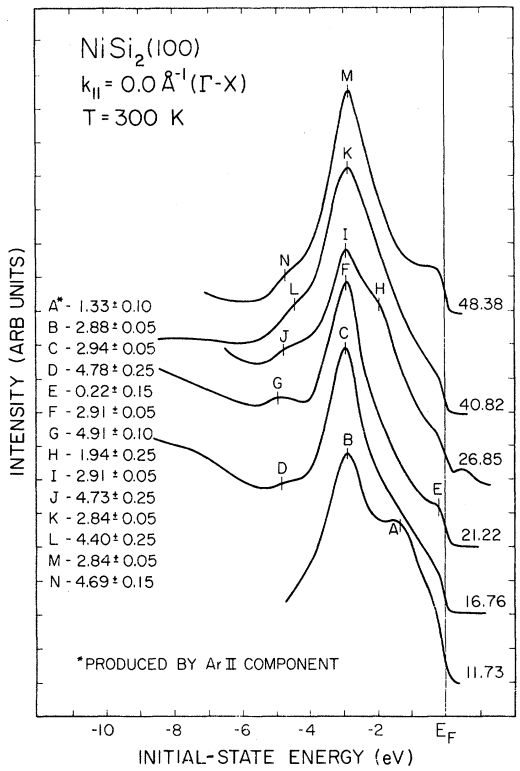

FIG. 2. Angle-resolved photoelectron energy distributions curves for $NiSi_2(100)$. Data were taken in normal emission geometry with $\Delta\Omega = 4°$. Energy resolution: $\hbar\omega = 43.38$ and 40.82 eV, $\Delta E_s \approx 200$ meV; other $\hbar\omega$, $\Delta E_s \approx 100$ meV. (Refer to Ref. 16 and text for a discussion of the origin of peak *A*.)

$NiSi_2(100)$. The EDC's were signal averaged until the statistical error was less than 2% for the four lower photon energies ($\hbar\omega \leq 26.85$ eV) and less than 5% for the higher photon energies ($\hbar\omega \geq 40.82$ eV).

Figure 3 illustrates the calculated band structure[4] for $NiSi_2$ along Δ and Λ directions of the bulk Brillouin zone. For cubic crystals, it has been shown[11,12] that, in normal emission geometry, only Δ_1 and Δ_5 symmetry initial states can be probed along Δ and only Λ_1 and Λ_3 symmetry initial states can be probed along Λ. Interpretation of our data is based on these selection rules and conservation laws associated with the photoemission process.

In the direct transition model of photoemission components of crystal momentum parallel to the surface k are conserved and electron energies are related by

$$E_f = E_i + \hbar\omega, \quad E = E_f - e\phi \ ,$$

where E_f and E_i are the final and initial states in the crystal, E is the kinetic energy of the photoemitted electron in vacuum, $\hbar\omega$ is the photon energy, and ϕ is the crystal work function. The final band disper-

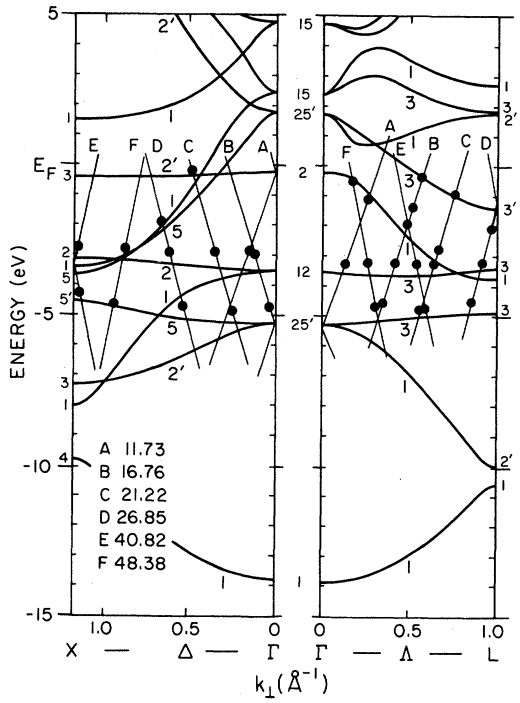

FIG. 3. Electronic structure of $NiSi_2$ along Γ-X and Γ-L of the bulk Brillouin zone (Ref. 2). Dots correspond to peaks in EDC's of Figs. 1 and 2. Lines through dots and letters indicate the final band and corresponding photon energies.

sion $E_f(k)$ can be determined experimentally,[13,14] but in many cases a single free-electron final band has been adequate to map the dispersion of initial-state bands. In this case the free-electron final-state band is given by

$$k=\frac{1}{\hbar}[2m(E+V_0)-\hbar^2k^2]^{1/2} ,$$

where V_0 is the crystal inner potential. In normal emission geometry, $k=0$ and a single parameter V_0 characterizes the final band. The free-electron final band used to place points on Fig. 3 corresponding to experimental data in Figs. 1 and 2 was determined by choosing V_0 to yield the best fit of our experimental results to the Λ_1 band which lies just below E_F at Γ and disperses downward to L. This procedure yields $V_0 \approx 14.2$ eV.

Peaks labeled *CFJMPS* and *GKNQT* in Fig. 1 correspond to the two Λ_3 (d character) bands; peaks labeled *BCFIKM* and *DGJLN* in Fig. 2 are also attributed to d character initial states with some caution regarding the emission process responsible for the peaks. Δ_1 and Δ_5 transitions are allowed, therefore the *DGJLN* peaks can be attributed to the Δ_5 band. Δ_2 transitions are forbidden, and therefore we attribute the structures labeled *BCFIKM* (particularly at photon energies away from Γ) to surface emission processes[15] which emphasize the high density of bulk states at -3.15 eV. Near Γ, significant contributions to the primary peak probably come from the Δ_1 band, and near X, significant contributions probably come from the Δ_1 and Δ_5 bands.

Our resonance lines were not monochromatized and this limits the resolution of spectra taken using the Ar I (11.73 eV) line,[16] and to a lesser extent, the Ne I (16.76 eV) line. The other lines can be regarded as highly monochromatic because the satellite lines are weak. We observed two cases where the Fermi edge appeared to be sharper and considerably higher for one crystal face compared to the other. These cases are represented by peak D in Fig. 1 and peak E in Fig. 2. We judged this behavior to indicate a direct transition and have included these points in Fig. 3.

Binding energies corresponding to the designated peaks are plotted in Fig. 3 at k values determined by the final band. Table I summarizes the critical-point energies obtained from our experimental results along with the values obtained from recent calculations.[4,5] Agreement is fairly good although the calculated d-band positions fall about 0.4 eV below our experimental results. Recent angle integrated photoemission studies[17] of polycrystalline $NiSi_2$ samples prepared by *in situ* fracturing are in excellent agreement with our results. In particular, the major d-band peaks (corresponding to a spatial average of the Δ_3 bands and Δ_2 and Δ_5 bands) are observed at 3.15 and 4.60 eV in the angle integrated spectra. Also, the relative peak intensities of the two flat Λ_3 bands are in good agreement with the projected d density of

TABLE I. Measured and calculated binding energies for $NiSi_2$ at several critical points in the bulk Brillouin zone. Linear-combination-of-Gaussian-orbital (LCGO) binding energies are from Ref. 4; linear augmented plane-wave (LAPW) binding energies are from Ref. 5.

Symmetry point	Binding energy	calculated	
	Experimental	LAPW[a]	LCGO[b]
$L_{3'}$	2.05 ±0.20	1.19	1.41
L_3 (upper)	3.13 ±0.10	3.48	3.46
L_3 (lower)	4.50 ±0.10	4.81	4.95
Γ_{12}	3.20 ±0.10	3.63	3.61
$\Gamma_{25'}$	4.90 ±0.10	5.19	5.29
$\Gamma_{2'}$	0.50 ±0.20	0.13	0.27
X_2	2.84 ±0.10	3.25	3.22
$X_{5'}$	4.40 ±0.20	4.31	4.63

[a] Reference 5. [b] Reference 4.

states obtained from both self-consistent[4,5] and extended Huckel[18] calculations.

ACKNOWLEDGMENTS

We would like to thank D. M. Bylander and L. Kleinman for helpful discussions and for providing us with their results prior to publication. We would like also to thank Chabel *et al.* and Francisoi *et al.* for sending us reports of their work prior to publication. This work was sponsored by the Joint Services Electronics Program (F496200-77-C-0101) and by the NSF under Grant No. DMR 79-23629.

---

[1]H. J. Goldschmidt, *Interstitial Compounds* (Plenum, New York, 1967).

[2]K. N. Tu, Appl. Phys. Lett. 27, 221 (1975).

[3]K. C. R. Chiu, J. M. Poate, L. C. Feldman, and C. J. Doherty, Appl. Phys. Lett. 36, 544 (1980).

[4]D. M. Bylander, L. Kleinman, K. Mednick, and W. R. Grise, Phys. Rev. B (in press).

[5]Y. J. Chabal, D. R. Hamann, J. E. Rowe, and M. Schlüter, Phys. Rev. B25, 7598 (1982).

[6]H. Ishiwara, K. Hikosaka, M. Nagatoma, and S. Furukowa, Surf. Sci. 86, 711 (1979).

[7]D. E. Eastman, J. Vac. Sci. Technol. 17, 492 (1980).

[8]I. Abbati, G. Rossi, L. Braicovich, I. Lindau, and W. E. Spicer, J. Appl. Phys. 52, 6994 (1981).

[9]It is interesting to note that our work function difference for $NiSi_2(100)$ and $NiSi_2(111)$ and the corresponding variation of Schottky barrier height [P. E. Schmid, P. S. Ho, and T. Y. Tan, J. Vac. Sci. Technol. 20, 688 (1982)] are of opposite sign. The differences are small and may not be significant, however, this behavior supports the point of view that interface structure is the key to the Schottky barrier height. When plotted on a graph of Schottky barrier heights vs ϕ [J. L. Freeouf, Solid State Commun. 33, 1059 (1980)] our results fall nicely on the line representing other silicides.

[10]J. L. Erskine, Phys. Rev. Lett. 45, 1446 (1980).

[11]J. Hermanson, Solid State Commun. 22, 9 (1977).

[12]W. Eberhardt and F. J. Himpsel, Phys. Rev. B 21, 5572 (1980).

[13]T. C. Chiang, J. A. Knapp, M. Aono, and D. E. Eastman, Phys. Rev. B 21, 3513 (1980).

[14]W. Eberhardt and E. W. Plummer, Phys. Rev. B 21, 3245 (1980).

[15]B. Fenerbacher and R. F. Willis, J. Phys. C 9, 169 (1976).

[16]In addition to a strong satellite, the Ar I doublet is only 1.6 eV from the Ar II doublet which is relatively strong. Therefore a strong peak line *C* in Fig. 1 will have a satellite 1.65 eV below it produced by Ar I. In Fig. 1, the satellite peak nearly masks a real peak labeled *A*.

[17]A. Francisoi, J. H. Weaver, and F. A. Schmidt (unpublished).

[18]O. Bisi and C. Calandra, J. Phys. C 14, 5479 (1981).